Rasip1 mediates Rap1 regulation of Rho in endothelial barrier function through ArhGAP29

Anneke Post, Willem-Jan Pannekoek, Sarah H. Ross, Ingrid Verlaan, Patricia M. Brouwer, and Johannes L. Bos[1]

Molecular Cancer Research, Centre for Biomedical Genetics and Cancer Genomics Netherlands, University Medical Center Utrecht, 3582 CG Utrecht, The Netherlands

Edited* by Tony Pawson, Samuel Lunenfeld Research Institute, Toronto, ON, Canada, and approved May 31, 2013 (received for review April 9, 2013)

Rap1 is a small GTPase regulating cell–cell adhesion, cell–matrix adhesion, and actin rearrangements, all processes dynamically coordinated during cell spreading and endothelial barrier function. Here, we identify the adaptor protein ras-interacting protein 1 (Rasip1) as a Rap1-effector involved in cell spreading and endothelial barrier function. Using Förster resonance energy transfer, we show that Rasip1 interacts with active Rap1 in a cellular context. Rasip1 mediates Rap1-induced cell spreading through its interaction partner Rho GTPase-activating protein 29 (ArhGAP29), a GTPase activating protein for Rho proteins. Accordingly, the Rap1–Rasip1 complex induces cell spreading by inhibiting Rho signaling. The Rasip1–ArhGAP29 pathway also functions in Rap1-mediated regulation of endothelial junctions, which controls endothelial barrier function. In this process, Rasip1 cooperates with its close relative ras-association and dilute domain-containing protein (Radil) to inhibit Rho-mediated stress fiber formation and induces junctional tightening. These results reveal an effector pathway for Rap1 in the modulation of Rho signaling and actin dynamics, through which Rap1 modulates endothelial barrier function.

The small GTPase Rap1 regulates both integrin-mediated and cadherin-mediated adhesions. Rap1 can increase cell adhesion by inducing the allosteric activation and clustering of integrins, thereby increasing cell–extracellular matrix (ECM) adhesion (1–3). Upon cell–ECM engagement, Rap1 induces cell spreading, due to increased cell protrusion and decreased cell contraction, indicating changes in actin dynamics (4, 5). In addition, Rap1 regulates both epithelial and endothelial cell–cell adhesion (6–11). Particularly the role of Rap1 in controlling endothelial cell junctions is important, as weakening of the endothelial barrier can result in pathologies such as chronic inflammation, atherosclerosis, and vascular leakage (12–14). Activation of Rap1 in endothelial cells results in stabilization of junctions and consequently increased barrier function through the recruitment of β-catenin, resulting in stabilization of vascular endothelial (VE)–cadherin at cell–cell junctions (15–18) and rearrangements of the actin cytoskeleton (6, 7, 19–21). These rearrangements of the actin cytoskeleton include the disruption of radial stress fibers and the induction of cortical actin bundles, and consequently a switch from discontinuous, motile junctions into linear, stable junctions (6–8, 20). Rap1 achieves this at least in part by regulating Rho-signaling (6, 7, 10, 19, 20). The molecular mechanism of how Rap1 regulates Rho, however, remains largely elusive, although the Rap1-effector Krev interaction trapped protein 1 (Krit-1)/cerebral cavernous malformations 1 protein (CCM1) has been proposed to be involved (15, 16, 22).

In this study, we identified a Rap1-signaling cascade, comprising ras-interacting protein 1 (Rasip1), ras-association and dilute domain-containing protein (Radil), and Rho GTPase-activating protein 29 (ArhGAP29), affecting both cell spreading and endothelial barrier function by regulating the Rho-signaling cascade.

Results

Rasip1 Mediates Rap1-Induced Spreading Without Affecting Adhesion. To investigate whether Rasip1 is involved in Rap1-induced cell spreading, we used A549 cells stably expressing the cAMP responsive Rap1 guanine nucleotide exchange factor (GEF), exchange protein directly activated by cAMP 1 (Epac1) (5). When treated with the Epac1-specific cAMP analog, 8-pCTP-2′-O-Me-cAMP (hereafter referred to as 007), to activate endogenous Rap, cells showed a twofold increase in cell area compared with untreated cells, as determined by pixels per cell, 3 h after replating on fibronectin (Fig. 1*A*). Previously, we established that this effect is mainly mediated by Rap1A (23). siRNA-mediated depletion of Rasip1 significantly reduced 007-induced spreading (Fig. 1*A*). This result was obtained with both a pool of siRNAs (spRasip1) as well as with four single siRNAs targeting Rasip1 (siRasip1 #1–4) (Fig. 1*A*). Furthermore, add back of a YFP–Rasip1 construct to cells treated with siRNA targeting the 3′UTR of Rasip1 mRNA (siRasip1 #2) rescued siRNA-mediated depletion of endogenous Rasip1 (Fig. 1*B*), excluding an off-target effect of the siRNA. Interestingly, overexpression of YFP–Rasip1 itself did not induce cell spreading, but required Rap1 activation to promote cell spreading (Fig. 1*B*).

To assess whether Rasip1 affects 007-induced spreading by regulating the activity of Rap1, we measured the amount of GTP-bound Rap1 after depletion of Rasip1. Whereas depletion of Epac1 reduced the amount of Rap1–GTP after 007 treatment, depletion of Rasip1 had no effect on Rap1–GTP levels (Fig. 1*C*), ruling out that Rasip1 mediates 007-induced spreading by affecting Rap1 activity. To exclude any possibility that Rasip1 mediates a Rap1-independent effect of Epac1, we induced spreading by overexpression of a constitutively active Rap1 mutant. Overexpression of HA–Rap1AV12 potently induced a nearly twofold increase in cell area (Fig. S1*A*). Depletion of Rasip1 abolished this effect (Fig. S1*A*), indicating that Rasip1 mediates Rap1A-induced cell spreading. To investigate whether Rasip1 is selective for Rap1-induced spreading, we induced spreading independently of Rap1 by expression of constitutively active T-lymphoma invasion and metastatis-inducing protein 1 (Tiam1) (C1199), a GEF for the small GTPase Rac1. This resulted in a 1.5-fold increase in cell area (Fig. S1*B*). However, this increase was insensitive to depletion of either Rap1A or Rasip1 (Fig. S1*B*). Together, these results indicate that Rasip1 functions specifically downstream of Rap1 in cell spreading.

As described previously, cell spreading is a multistep process including the initiation and formation of cell–ECM contacts and induction of cytoskeletal rearrangements. Rap1 has been reported to both increase integrin affinity and induce integrin clustering, resulting in increased cell adhesion (1–3). We therefore investigated whether Rasip1 affects Rap1-induced cell spreading by mediating Rap1-induced cell–ECM interactions. First, we tested

Author contributions: A.P., W.-J.P., and J.L.B. designed research; A.P., W.-J.P., S.H.R., I.V., and P.M.B. performed research; A.P., W.-J.P., S.H.R., I.V., P.M.B., and J.L.B. analyzed data; and A.P., W.-J.P., and J.L.B. wrote the paper.

The authors declare no conflict of interest.

*This Direct Submission article had a prearranged editor.

Freely available online through the PNAS open access option.

[1]To whom correspondence should be addressed. E-mail: J.L.Bos@umcutrecht.nl.

This article contains supporting information online at www.pnas.org/lookup/suppl/doi:10.1073/pnas.1306595110/-/DCSupplemental.

CELL BIOLOGY

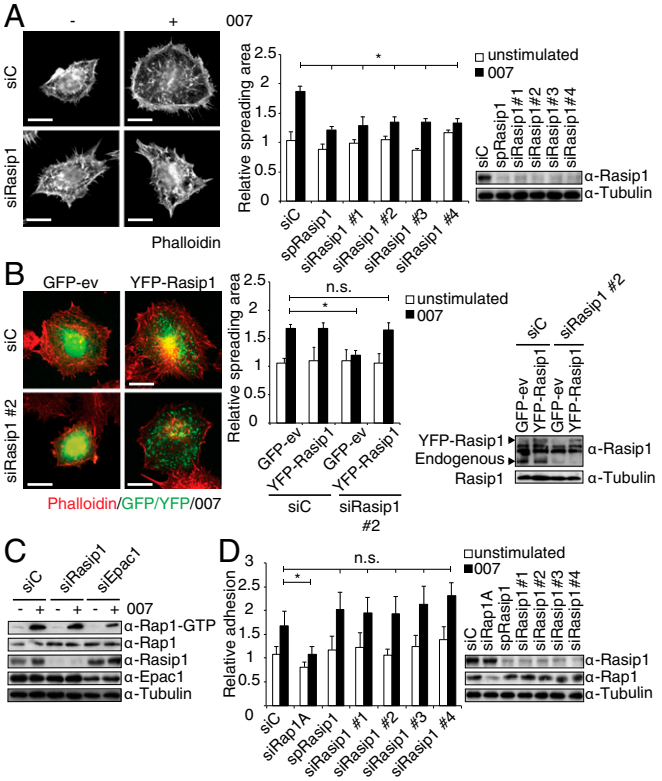

Fig. 1. Rasip1 mediates Rap1-induced cell spreading. (*A*, *Left*) Spreading of A549–Epac1 cells transfected with scrambled siRNA (siC) or a SMARTpool of siRNAs targeting Rasip1 (spRasip1). Cells were replated for 3 h on fibronectin-coated coverslips in the absence (–) or presence (+) of 100 μM 007. Cells were fixed and the actin cytoskeleton was stained with phalloidin. (*Right*) Quantification of cell area of A549–Epac1 cells transfected with scrambled siRNA (siC), a SMARTpool siRNAs targeting Rasip1 (spRasip1), or single siRNAs targeting Rasip1 (siRasip1 #1–4) in the absence (unstimulated) or presence (007) of 007, as quantified using ImageJ. Depicted is average spreading area ± SD of three individual experiments and a minimum of 10 cells per experiment, normalized to unstimulated, siC-transfected cells. $*P < 0.05$. Knockdown efficiency was determined by Western blot. (*B*) Recovery of Rasip1 depletion by an siRNA-resistant YFP–Rasip1 construct. A549–Epac1 cells were treated with siC or siRasip1 #2 16 h before cotransfection with either GFP–empty vector (GFP-ev) or siRNA-resistant YFP–Rasip1 construct. Cells were replated, treated, and quantified as for *A*. Depicted is average spreading area ± SD of three individual experiments normalized to unstimulated siC-transfected cells. $*P < 0.02$. Knockdown efficiency was determined by Western blot. (*C*) Pull-down of Rap1–GTP from A549–Epac1 cells, either unstimulated (–) or upon 15 min stimulation with 100 μM 007 (+), transfected with siC, siRasip1, or siEpac1. (*D*) Adhesion of A549–Epac1 cells transfected with siC, siRasip1, or single siRNAs targeting Rasip1 (siRasip1 #1–4). Cells were replated onto fibronectin-coated surfaces for 25 min in the absence (unstimulated) or presence (007) of 100 μM 007. Nonadherent cells were washed off and adherent cells were quantified by measuring endogenous phosphatase activity. Depicted are mean data ± SD of five individual experiments normalized to unstimulated siC-transfected cells. $*P < 0.03$. Knockdown efficiency was determined by Western blot. All statistical analyses were obtained by performing a paired Student *t* test. n.s., not significant. (Scale bar, 20 μM.)

whether Rasip1 is involved in Rap1-induced adhesion. For this, we assessed the amount of cells adherent to fibronectin over a 25-min period in the presence or absence of 007. In scrambled siRNA-treated cells, 007 induced a 1.5-fold increase in cell adhesion (Fig. 1*D*). As expected, siRap1A abolished this effect. However, depletion of Rasip1 did not affect 007-induced adhesion (Fig. 1*D*). These results indicate that in A549–Epac1 cells Rasip1 specifically mediates cell spreading without affecting cell adhesion. Importantly, focal adhesions formed and matured normally as determined by Paxillin, pY118–Paxillin, and Vinculin staining (Fig. S1*C*), suggesting that depletion of Rasip1 does not affect cell spreading through inhibition of the focal adhesion maturation.

Full-Length Rasip1 Interacts with Active Rap1. Mitin et al. (24) showed that the ras-association (RA) domain of Rasip1 can interact with the constitutively active Rap1A63E mutant in vitro. Furthermore, both Rap1 and Rasip1 have been reported to localize to the perinuclear region (Fig. 1*B*) (24, 25). Together with our results that show that Rasip1 functions downstream from Rap1, this prompted us to investigate whether full-length Rasip1 and Rap1 interact in vivo. To that end, we measured Rasip1–Rap1 interaction by Förster resonance energy transfer (FRET), using the acceptor photobleaching technique. Cells were transfected with GFP–Rasip1 and either the constitutively active mCherry–Rap1V12 or inactive mCherry–Rap1N17. FRET was observed between GFP–Rasip1 and mCherry–Rap1V12 (Fig. 2*A*) with an efficiency of ∼19% versus an efficiency of ∼2.5% for GFP–Rasip1 and mCherry–Rap1N17 (Fig. 2*B*), indicating that Rasip1 and active Rap1 indeed interact within the cell.

Rasip1 Mediates Rap1-Induced Spreading by Affecting Rho Signaling Through the RhoGAP ArhGAP29. Rasip1 has previously been reported to inhibit RhoA signaling through interaction with the RhoGAP ArhGAP29 (26). We were able to confirm this interaction (Fig. S2*A*), and we therefore determined whether Rap1-induced cell spreading also requires ArhGAP29. Indeed, depletion of ArhGAP29 also inhibited 007-induced spreading of A549–Epac1 cells (Fig. 3*A*). Furthermore, as we have demonstrated for Rasip1, depletion of ArhGAP29 does not abolish 007-induced initial adhesion (Fig. 3*B*). These results indicate that Rap1-induced cell spreading requires the Rasip1–ArhGAP29 complex.

ArhGAP29 has been shown to have predominant GTPase activating protein (GAP) activity toward the small GTPase RhoA over Rac1 and Cdc42 (27). Activation of Rho results in increased activity of its effector Rho-associated protein kinase (ROCK), which phosphorylates myosin light chain 2 (MLC2) and myosin phosphatase targeting subunit 1 (MYPT1), resulting in increased actomyosin contraction. During the process of cell spreading, cell contraction must be reduced to allow cell spreading

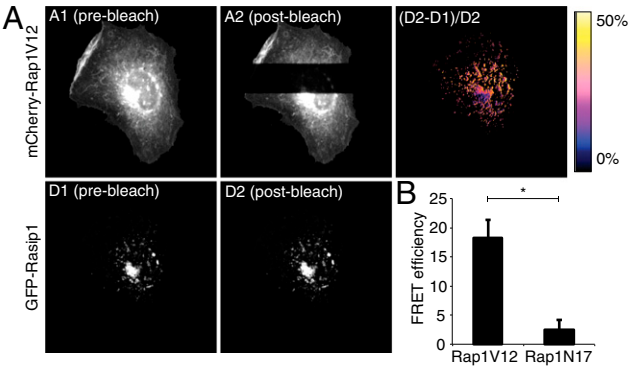

Fig. 2. Rasip1 interacts with active Rap1. Analysis of FRET between GFP–Rasip1 and mCherry–Rap1V12 or mCherry–Rap1N17 using acceptor photobleaching. (*A*) Scans of GFP–Rasip1 (donor) and mCherry–Rap1V12 (acceptor) were taken before (pre-) and after (post-) photobleaching, and FRET efficiency was calculated by $E = (Donor_{post} - Donor_{pre})/Donor_{post}$. (*B*) Average FRET efficiency calculated for GFP–Rasip1 and mCherry–Rap1V12 or GFP–Rasip1 and mCherry–Rap1N17. Intensities were calculated with ImageJ within a defined region of interest (ROI). Per cell three ROIs were taken of both the bleached area and unbleached area for background correction, and values were averaged. Three cells per experiment were visualized. Graph depicts the mean FRET efficiency of three individual experiments ± SD. Statistical analysis was obtained by performing a paired Student *t* test. $*P < 0.01$.

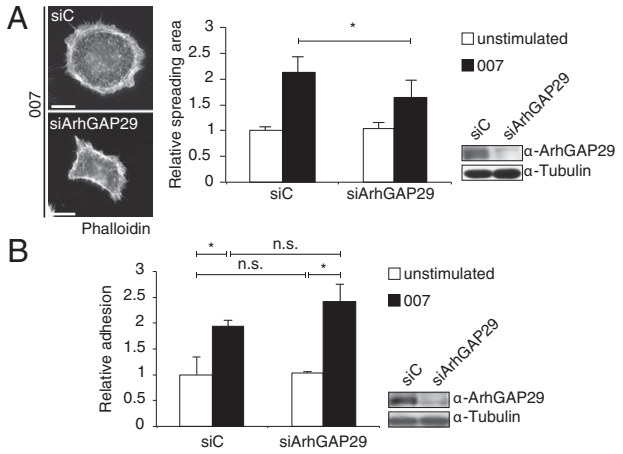

Fig. 3. ArhGAP29 mediates Rap1-induced spreading. (*A*) Spreading of A549–Epac1 cells treated with scrambled siRNA (siC) or siRNA targeting ArhGAP29 (siArhGAP29). Cells were replated, treated, and quantified as for Fig. 1*A*. Depicted is average spreading area ± SD of five individual experiments normalized to unstimulated siC-transfected cells. Knockdown efficiency was determined by Western blot. *$P < 0.005$. (*B*) Adhesion of A549–Epac1 cells transfected with siC or siArhGAP29. Cells were replated, treated, and quantified as for Fig. 1*D*. Depicted are mean data ± SD of three individual experiments normalized to unstimulated, siC-transfected cells. *$P < 0.01$. All statistical analyses were obtained by performing a paired Student *t* test. n.s., not significant. (Scale bar, 20 μM.)

to occur (28, 29). To assess whether Rap1 induces cell spreading by reducing cell contraction, A549–Epac1 cells, adherent to fibronectin, were stimulated with 007 for 30 min. Cells were lysed and assessed for phosphorylated MLC2 (pMLC2) levels. Treatment with 007 reduced the levels of pMLC2, and depletion of either Rasip1 or ArhGAP29 attenuated the 007-induced reduction of pMLC2 (Fig. 4*A*). These results indicate that Rap1 induces cell spreading by reducing the amount of phosphorylated MLC2. Furthermore, because Rasip1 and ArhGAP29 depletion attenuates this effect, we concluded that this effect is achieved through reduction of Rho activity.

To address the notion that the Rap1–Rasip1–ArhGAP29 pathway affects cell spreading through modulation of Rho activity, we hypothesized that if the effect of Rasip1 and ArhGAP29 depletion on Rap1-induced spreading is due to increased levels of Rho activity, inhibition of Rho activity should alleviate the inhibitory effects of Rasip1 and ArhGAP29 depletion on Rap1-induced spreading. We therefore treated A549–Epac1 cells with the Rho inhibitor C3 transferase. Indeed, whereas depletion of Rasip1 or ArhGAP29 inhibited 007-induced spreading, treatment with C3 transferase not only induced cell spreading on its own but also relieved the inhibitory effect of depletion of Rasip1 or ArhGAP29 on 007-induced spreading (Fig. 4 *B* and *C*, Fig. S2 *B* and *C*). Furthermore, the ROCK inhibitor Y27623 relieved the inhibitory effect of ArhGAP29 depletion on 007-induced cell spreading (Fig. 4*C*, Fig. S2*C*). Conversely, overexpression of a constitutively active RhoA (RhoAQ63L) mutant inhibited 007-induced spreading (Fig. S2*D*), indicating that RhoA activity must be reduced to allow Rap1-induced spreading to occur. Taken together, we conclude that Rap1, through Rasip1 and ArhGAP29, reduces Rho activity and consequently actomyosin-induced tension.

Rasip1 and ArhGAP29 Mediate Rap1-Induced Endothelial Barrier Function. To investigate the physiological relevance of the Rap1–Rasip1–ArhGAP29 signaling pathway, we investigated its involvement in Rap1-induced endothelial barrier function. First, we determined whether Rasip1 and ArhGAP29 were also involved in cell spreading in endothelial cells. In human umbilical vein endothelial cells (HUVECs), depletion of either Rasip1 or ArhGAP29 abrogated 007-induced spreading (Fig. S3*A*), demonstrating that the Rap1–Rasip1–ArhGAP29 pathway is conserved in endothelial cells. Previously, it was demonstrated that depletion of Rap1 in HUVECs results in both reduced basal and 007-induced endothelial barrier function, as measured by electrical impedance to evaluate the junctional resistance (R_b) (8, 9). In a confluent monolayer of HUVECs, we found that depletion of ArhGAP29 decreased basal resistance and 007-induced resistance compared with scrambled siRNA-treated cells (Fig. 5*A*), thereby phenocopying previous results for Rap1 knockdown (8, 9). Epac1 has been shown to regulate endothelial barrier function in a Rap1-dependent and -independent manner (8, 21). To determine whether ArhGAP29 mediates the Rap1-dependent component of Epac1-regulated barrier function, we induced endothelial barrier function in an Epac1-independent, Rap1A-dependent manner. For this, we transduced HUVECs with the constitutively active mutant of Rap1A, Rap1AV12. Overexpression of Rap1AV12 increased the impedance compared with empty vector-transfected cells (Fig. 5*B*). When ArhGAP29 was depleted, overexpression of Rap1AV12 was no longer able to increase the electrical impedance (Fig. 5*B*), confirming that ArhGAP29 mediates Rap1A-induced endothelial barrier function.

Depletion of Rasip1 also significantly reduced the basal endothelial barrier function, but the effect was clearly much less dramatic than depletion of ArhGAP29 (Fig. 5*C*). This suggested that Rasip1 might not be the only mediator of Rap1 controlling

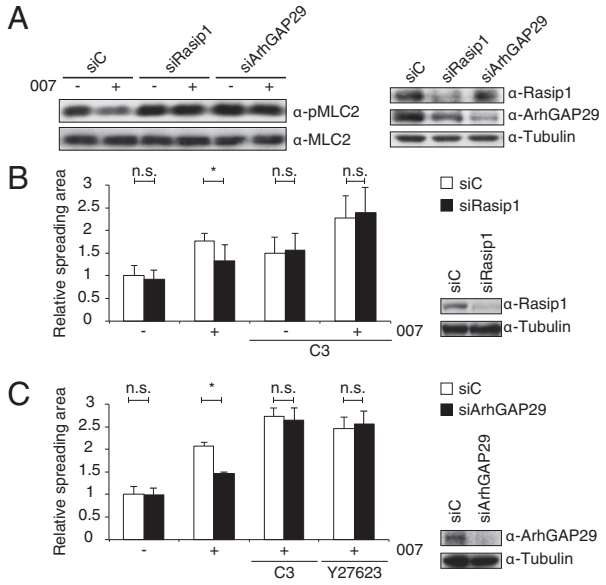

Fig. 4. Rap1 modulates Rho activity through Rasip1 and ArhGAP29. (*A*) Phosho–MLC2 (pMLC2) levels in A549–Epac1 cells transfected with siC, siRasip1, or siArhGAP29. Upon 30 min stimulation with 100 μM 007 (+), cells were lysed and lysates were subjected to Western blotting. Minus depicts untreated cells. Western blot is a representative of four individual experiments. (*B*) Quantification of spreading of A549–Epac1 cells transfected with siC or siRasip1 in the presence or absence of 007 and C3 transferase (C3). Cells were replated, fixed, and quantified as for Fig. 1*A*. Depicted is average spreading area ± SD of four individual experiments normalized to unstimulated siC-transfected cells. Knockdown efficiency was determined by Western blot. *$P < 0.008$. Immunofluorescent images are depicted in Fig. S2*B*. (*C*) Quantification of spreading of A549–Epac1 cells transfected with siC or siArhGAP29 in the presence or absence of 007 and C3 transferase (C3) or a ROCK inhibitor (Y27623). Cells were replated, fixed, and quantified as for Fig. 1*A*. Depicted is average spreading area ± SD of three individual experiments normalized to unstimulated siC-transfected cells. Knockdown efficiency was determined by Western blot. *$P < 0.005$. Immunofluorescent images are depicted in Fig. S2*B*. n.s., not significant.

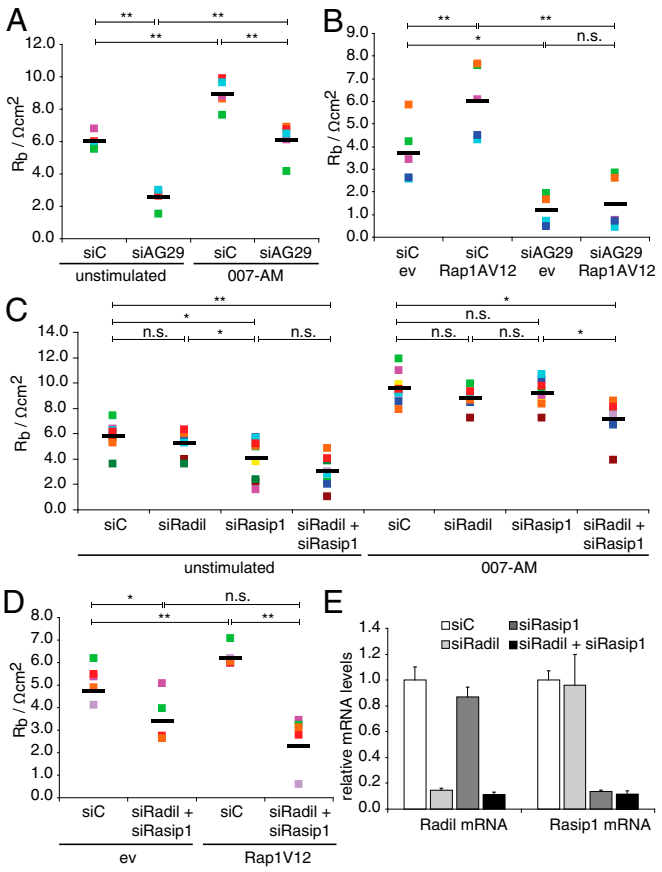

Fig. 5. Rasip1, Radil, and ArhGAP29 mediate Rap1-induced endothelial barrier function. (*A*) Endothelial barrier (R_b) of control HUVEC monolayers (siC) and HUVEC monolayers depleted of ArhGAP29 (siAG29), as determined by ECIS, both before and after the addition of 1 μM 8-pCPT-2′-O-Me-cAMP-acetoxymethyl (007-AM). Different colors represent independent experiments (n = 5). Averages are indicated by the black lines. (*B*) Endothelial barrier (R_b) of control HUVEC monolayers (siC) and HUVEC monolayers depleted of ArhGAP29 (siAG29), transduced with control lentivirus or Rap1AV12 containing lentivirus. Different colors represent independent experiments (n = 5). Averages are indicated by the black lines. (*C*) Endothelial barrier (R_b) of control HUVEC monolayers (siC) and HUVEC monolayers depleted of Radil (siRadil), Rasip1 (siRasip1), or both (siRadil + siRasip1), both before and after the addition of 1 μM 007-AM. Different colors represent independent experiments (n = 10). Averages are indicated by the black lines. (*D*) Endothelial barrier (R_b) of control HUVEC monolayers (siC) and HUVEC monolayers depleted of both Radil and Rasip1 (siRadil + siRasip1), transduced with control lentivirus or Rap1AV12 containing lentivirus. Different colors represent independent experiments (n = 6). Averages are indicated by the black lines. (*E*) HUVECs depleted of Radil (siRadil), Rasip1 (siRasip1), or both (siRadil + siRasip1) were grown to confluency, after which RNA was extracted and mRNA levels were assessed by real-time quantitative PCR. The histogram shows Radil and Rasip1 expression within one of the experiments represented in Fig. 6*C*. Expression was correlated to the expression in siC-transfected cells. Error bars indicate SD between PCR triplicates. All statistical analyses were obtained by performing a paired Student t test. $^{**}P < 0.01$, $^{*}P < 0.05$, n.s., not significant.

ArhGAP29. Indeed, recently Radil, a close relative of Rasip1, was found to interact with ArhGAP29 in a mass spectometry analysis (30). In addition, Radil is also identified as an effector of Rap1 required for Rap1-induced cell spreading (23, 31) (Fig. S3*A* and *B*) and like Rasip1 and ArhGAP29, is dispensable for 007-induced cell adhesion (Fig. S3*C*). We therefore investigated the contribution of Radil to Rap1-induced endothelial barrier function. Whereas depletion of Radil did not significantly affect endothelial barrier function, simultaneous depletion of Rasip1 and Radil did reduce the endothelial barrier resistance to a similar level as depletion of ArhGAP29, both in the absence or presence of 007 (Fig. 5 *C* and *E*). Furthermore, simultaneous depletion of Rasip1 and Radil prevented the induction of resistance by the overexpression of Rap1AV12 (Fig. 5*D*), indicating that Rasip1 and Radil together specifically mediate the Rap1-dependent component of Epac1-induced endothelial barrier function.

Rap1–Rasip1–ArhGAP29 Axis Induces Endothelial Barrier Function Through Rho. To confirm that the Rap1–Rasip1–ArhGAP29 signaling pathway regulates endothelial barrier function through Rho signaling, we investigated whether depletion of Rho could alleviate the endothelial barrier dysfunction caused by ArhGAP29 depletion. Depletion of either RhoA, RhoB, or RhoC slightly increased endothelial barrier resistance, however simultaneous depletion of RhoA, RhoB, and RhoC resulted in a robust increase in endothelial barrier function (Fig. S4*A*), indicating that a reduction of Rho activity increases endothelial barrier function. The reduction in endothelial barrier resistance upon ArhGAP29 depletion, both in the absence and presence of 007, was completely restored by simultaneous depletion of Rho (Fig. 6*A*).

The induction of endothelial barrier function by activation of the Epac1–Rap1 signaling pathway is accompanied by actin cytoskeletal rearrangements, including induction of junctional actin formation and reduction of radial stress fibers (6–8, 20). Radial stress fibers attach to and exert tension on adherens junctions (AJs), resulting in irregular junctions, which is regulated by the Rho–Rock signaling pathway (32, 33). Indeed, depletion of RhoA, RhoB, and RhoC resulted in the loss of radial stress fibers and induced linear AJs, which was visualized by staining of β-catenin (Fig. 6*B*). As reported previously (6–8, 20), activation of Epac1 also resulted in a transition from irregular to more linear junctions, accompanied by a reduction of radial stress fibers (Fig. 6*C*). Interestingly, simultaneous knockdown of Rasip1 and Radil or depletion of ArhGAP29 resulted in an increased number of irregular junctions and showed an increased stress fiber profile (Fig. 6*C*, Fig. S4 *C* and *D*), suggesting increased tension on the AJs. Moreover, cells overexpressing ArhGAP29 lacked radial stress fibers (Fig. 6*D*), thereby phenocopying Rho depletion. Together, these results show that ArhGAP29 mediates Rap1-induced endothelial barrier function through Rho signaling, thereby reducing actomyosin-induced tension on AJs.

Discussion

Here we identified a signaling cascade regulated by Rap1, through which Rap1 regulates Rho signaling and actomyosin-induced tension, resulting in cell spreading and endothelial barrier function. Specifically, we identified Rasip1 as a Rap1-effector, interacting with active Rap1 and mediating Rap1-induced cell spreading and endothelial barrier function. Furthermore, we found that the Rasip1 homolog and Rap1 effector, Radil, was similarly involved in Rap1-induced endothelial barrier function. The common binding partner of both Rasip1 (34) and Radil (30), ArhGAP29, was also required for Rap1-mediated cell spreading and endothelial barrier function, indicating that this protein is part of the effector complex regulated by Rap1. ArhGAP29 has GAP activity toward RhoA (27) and was previously found to inhibit Rho signaling (26). Indeed, Rap1 activation resulted in reduced phosphorylated MLC2 levels, and this required Rasip1 and ArhGAP29. Inhibition of Rho or ROCK activity attenuated the 007-induced spreading defect in cells depleted of Rasip1 or ArhGAP29. Furthermore, simultaneous depletion of Rho proteins rescued the effect of ArhGAP29 depletion on endothelial barrier function. We were, however, unable to demonstrate consistent reduction in Rho–GTP levels upon Rap1 activation (Fig. S5), perhaps because Rho activity is only locally affected. Indeed, several recent reports emphasize the importance of spatiotemporal

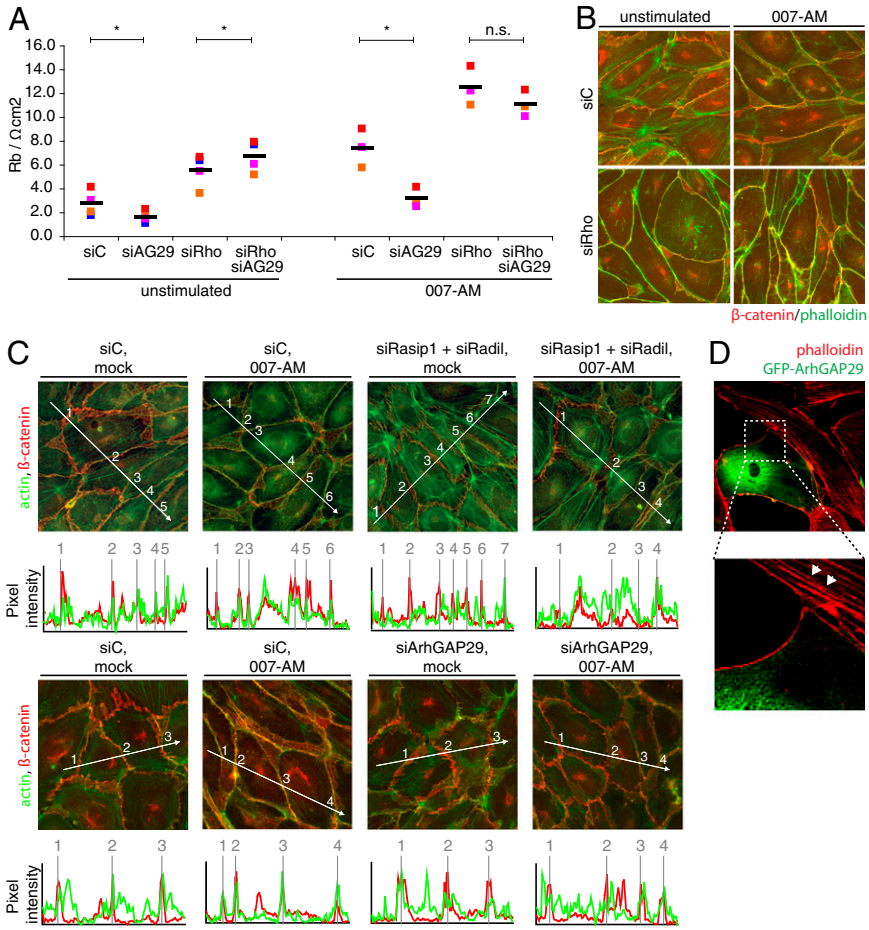

Fig. 6. Rasip1, Radil, and ArhGAP29 mediate Rap1-regulation of Rho in endothelial barrier function. (*A*) Endothelial barrier (R_b) of control HUVEC monolayers (siC) and HUVEC monolayers depleted of ArhGAP29 (siAG29), RhoA, RhoB, and RhoC (siRho) or ArhGAP29 and RhoA, RhoB, and RhoC (siAG29 + siRho), both before and after the addition of 1 μM 007-AM. Different colors represent independent experiments ($n = 4$). Averages are indicated by the black lines. A Western blot to determine knockdown efficiency is depicted in Fig. S4*B*. *$P < 0.04$. n.s., not significant. (*B*) Immunofluorescence of confluent HUVEC monolayers transfected with control (siC) or RhoA, RhoB, and RhoC (siRho) siRNA. Monolayers were stimulated with or without 007-AM (1 μM, 10 min) and stained for F-actin (phalloidin, green) and β-catenin (red). (*C*, *Upper*) Immunofluorescence of confluent HUVEC monolayers transfected with control (siC), Rasip1 and Radil (siRasip1 + siRadil) or ArhGAP29 (siArhGAP29) siRNA. Monolayers were stimulated with or without 007-AM (1 μM, 10 min) and stained for F-actin (phalloidin, green) and β-catenin (red). (*Lower*) The graphs show profiles of fluorescence signal intensities along the line scan of phalloidin (green) and β-catenin (red) staining. Gray lines and numbers indicate where the line scan crosses an AJ. (*D*) Immunofluoresence of HUVECs transduced with GFP–ArhGAP29 containing lentivirus. Cells were fixed and the actin cytoskeleton was stained with phalloidin (red). Arrowheads depict radial stress fibers.

regulation of Rho activity in a variety of biological processes, including endothelial barrier function (35–39).

Previously, it has been described that Rho-induced formation and contraction of radial stress fibers, attached to VE–cadherin–based AJs, induce irregular, highly dynamic junctions, resulting in increased endothelial permeability (32, 33). Compatible with this notion, depletion of ArhGAP29 or Rasip1 and Radil increased the amount of stress fibers and irregular junctions. In contrast, overexpression of ArhGAP29 resulted in complete loss of radial stress fibers, thereby phenocopying cells devoid of RhoA, RhoB, and RhoC. We therefore conclude that Rasip1 is an effector of Rap1 that together with Radil controls Rho signaling through ArhGAP29 in cell spreading and endothelial barrier function, and that this is achieved by the reduction of actomyosin-induced tension (Fig. S6).

In apparent contrast to previous reports (26, 31), we find that Rasip1, Radil, and ArhGAP29 are dispensable for Rap1-induced initial cell adhesion, suggesting that Rap1 can differentially regulate cell adhesion and cell spreading (Fig. S6). However, we did observe that the number of focal adhesions per cell was reduced in Rasip1- or Radil-depleted cells (Fig. S1*C*) (23), possibly accounting for the reduced amount of active integrins found previously when depleting Rasip1 (26) or Radil (31). Our finding that Rasip1 and Radil did not affect Rap1-induced initial adhesion does imply that other Rap1 effectors are involved in this process. Several different Rap effectors have been identified that play a role in Rap1-induced cell adhesion and integrin regulation, such as Rap1–GTP-interacting adaptor molecule (Riam) and regulator for adhesion and polarization enriched in lymphoyd tissues (RapL). For the A549-Epac1 cells, however, the effector for Rap1-induced initial adhesion is currently elusive.

The interplay between Rasip1 and Radil requires further investigation. Interestingly, Radil might interact with ArhGAP29 through its PDZ (PSD-95/Dlg/ZO1) domain (30), a domain not present in Rasip1. Perhaps Radil and Rasip1 form a complex, with Radil as the ArhGAP29 binding partner.

Endothelial junctions are regulated by a number of signaling pathways, one of which is the Rap1–Rasip1/Radil–ArhGAP29–Rho pathway. However, Rap1 may use additional routes for controlling these junctions. As already indicated, the Krit-1/CCM1 route may be one of them. Furthermore, in epithelial cells Rap1

localizes nonmuscle myosin II-B to cortical actin bundles in a Rho-independent manner (40).

Materials and Methods

A detailed description of the experimental procedures and of all compounds used can be found in *SI Material and Methods*.

Spreading Assays, Short-Term Adhesion Assays, and Immunofluorescence. Cells were trypsinized and kept in suspension for 1.5 h to allow surface proteins to recover. For spreading assays, cells were replated onto fibronectin-coated coverslips and allowed to adhere for 3 h at 37 °C. Cells were fixed and incubated with appropriate antibodies, and immunofluorescent images were obtained. For short-term adhesion assays, cells were replated onto fibronectin-coated cell culture dishes and allowed to adhere for 25 min at 37 °C. Unbound cells were discarded by washing with PBS, after which adhered cells were lysed in alkaline phosphatase buffer and the total amount of cellular protein was determined by measuring absorption at 405 nm. For evaluation of confluent HUVEC monolayers, HUVECs were plated onto fibronectin-coated glass coverslips and grown to confluency. After stimulation, cells were fixed and incubated with appropriate antibodies and immunofluorescent images were obtained. ImageJ (National Institutes of Health) was used to quantify images. *P* values were determined by Student *t* test (two-tailed, paired).

Rap Activation Assay. Cells were stimulated for 15 min with 100 μM 007, and subsequently lysed in Ralbuffer. Active Rap was precipitated with a GST fusion protein of the Ras-binding domain of Ral guanine nucleotide dissociation stimulator precoupled to glutathione–Sepharose beads. Bound proteins were eluted in Laemmli buffer and analyzed by SDS/PAGE and Western blotting.

Acceptor-Photobleaching–Based FRET Detection. Cells expressing mCherry–Rap1V12, mCherry–Rap1N17, or GFP–Rasip1 were plated onto fibronectin-coated coverslips as described for the spreading assays. FRET efficiency was determined by the acceptor-photobleaching method. A series of prebleaching and postbleaching fluorescence intensities of GFP (donor) were recorded and the energy transfer efficiency (E) was calculated from the equation: $E = (D_{post} - D_{pre})/D_{post.}$ Intensities were calculated with ImageJ. Statistical analysis was obtained by performing a paired Student *t* test.

Endothelial Barrier Measurements. Endothelial barrier was assessed by Electrical Cell Impedance Sensing (ECIS) measurements. HUVECs were plated onto fibronectin-coated electrodes and grown to confluency. The impedance was measured at multiple frequencies within the range of 62.5 Hz to 16,000 Hz at 37 °C. These frequency scans were used to calculate endothelial barrier (R_b). *P* values were calculated by Student *t* test (two-tailed, paired).

ACKNOWLEDGMENTS. We thank Prof. Dr. K. Kariya, Dr. J. de Rooij, and Dr. J. G. Collard for providing DNA constructs and members of the J.L.B. laboratory for discussions. A.P. and W.-J.P. were funded by grants from the Dutch Cancer Society (Koningin Wilhelmina Fonds voor de Nederlandse Kankerbestrijding). S.H.R. was supported by a Federation of European Biochemical Societies Long-Term Fellowship. This work was further supported by the Netherlands Genomics Initiative of the Netherlands Organization for Scientific Research (Netherlands Organization for Scientific Research).

1. Katagiri K, Maeda A, Shimonaka M, Kinashi T (2003) RAPL, a Rap1-binding molecule that mediates Rap1-induced adhesion through spatial regulation of LFA-1. *Nat Immunol* 4(8):741–748.
2. Lafuente EM, et al. (2004) RIAM, an Ena/VASP and Profilin ligand, interacts with Rap1-GTP and mediates Rap1-induced adhesion. *Dev Cell* 7(4):585–595.
3. Lee HS, Lim CJ, Puzon-McLaughlin W, Shattil SJ, Ginsberg MH (2009) RIAM activates integrins by linking talin to ras GTPase membrane-targeting sequences. *J Biol Chem* 284(8):5119–5127.
4. Lyle KS, Raaijmakers JH, Bruinsma W, Bos JL, de Rooij J (2008) cAMP-induced Epac-Rap activation inhibits epithelial cell migration by modulating focal adhesion and leading edge dynamics. *Cell Signal* 20(6):1104–1116.
5. Ross SH, et al. (2012) Rap1 can bypass the FAK-Src-Paxillin cascade to induce cell spreading and focal adhesion formation. *PLoS ONE* 7(11):e50072.
6. Cullere X, et al. (2005) Regulation of vascular endothelial barrier function by Epac, a cAMP-activated exchange factor for Rap GTPase. *Blood* 105(5):1950–1955.
7. Kooistra MR, Corada M, Dejana E, Bos JL (2005) Epac1 regulates integrity of endothelial cell junctions through VE-cadherin. *FEBS Lett* 579(22):4966–4972.
8. Pannekoek WJ, et al. (2011) Epac1 and PDZ-GEF cooperate in Rap1 mediated endothelial junction control. *Cell Signal* 23(12):2056–2064.
9. Wittchen ES, Aghajanian A, Burridge K (2011) Isoform-specific differences between Rap1A and Rap1B GTPases in the formation of endothelial cell junctions. *Small GTPases* 2(2):65–76.
10. Wittchen ES, et al. (2005) Rap1 GTPase inhibits leukocyte transmigration by promoting endothelial barrier function. *J Biol Chem* 280(12):11675–11682.
11. Knox AL, Brown NH (2002) Rap1 GTPase regulation of adherens junction positioning and cell adhesion. *Science* 295(5558):1285–1288.
12. Baluk P, Hashizume H, McDonald DM (2005) Cellular abnormalities of blood vessels as targets in cancer. *Curr Opin Genet Dev* 15(1):102–111.
13. Bazzoni G, Dejana E (2004) Endothelial cell-to-cell junctions: Molecular organization and role in vascular homeostasis. *Physiol Rev* 84(3):869–901.
14. Weis SM (2008) Vascular permeability in cardiovascular disease and cancer. *Curr Opin Hematol* 15(3):243–249.
15. Glading A, Han J, Stockton RA, Ginsberg MH (2007) KRIT-1/CCM1 is a Rap1 effector that regulates endothelial cell cell junctions. *J Cell Biol* 179(2):247–254.
16. Glading AJ, Ginsberg MH (2010) Rap1 and its effector KRIT1/CCM1 regulate beta-catenin signaling. *Dis Model Mech* 3(1-2):73–83.
17. Lorenowicz MJ, Fernandez-Borja M, Kooistra MR, Bos JL, Hordijk PL (2008) PKA and Epac1 regulate endothelial integrity and migration through parallel and independent pathways. *Eur J Cell Biol* 87(10):779–792.
18. Noda K, et al. (2010) Vascular endothelial-cadherin stabilizes at cell-cell junctions by anchoring to circumferential actin bundles through alpha- and beta-catenins in cyclic AMP-Epac-Rap1 signal-activated endothelial cells. *Mol Biol Cell* 21(4):584–596.
19. Birukova AA, et al. (2010) Rac GTPase is a hub for protein kinase A and Epac signaling in endothelial barrier protection by cAMP. *Microvasc Res* 79(2):128–138.
20. Fukuhara S, et al. (2005) Cyclic AMP potentiates vascular endothelial cadherin-mediated cell-cell contact to enhance endothelial barrier function through an Epac-Rap1 signaling pathway. *Mol Cell Biol* 25(1):136–146.
21. Sehrawat S, Cullere X, Patel S, Italiano J, Jr., Mayadas TN (2008) Role of Epac1, an exchange factor for Rap GTPases, in endothelial microtubule dynamics and barrier function. *Mol Biol Cell* 19(3):1261–1270.
22. Stockton RA, Shenkar R, Awad IA, Ginsberg MH (2010) Cerebral cavernous malformations proteins inhibit Rho kinase to stabilize vascular integrity. *J Exp Med* 207(4):881–896.
23. Ross SH, et al. (2011) Ezrin is required for efficient Rap1-induced cell spreading. *J Cell Sci* 124(Pt 11):1808–1818.
24. Mitin NY, et al. (2004) Identification and characterization of rain, a novel Ras-interacting protein with a unique subcellular localization. *J Biol Chem* 279(21):22353–22361.
25. Ohba Y, Kurokawa K, Matsuda M (2003) Mechanism of the spatio-temporal regulation of Ras and Rap1. *EMBO J* 22(4):859–869.
26. Xu K, et al. (2011) Blood vessel tubulogenesis requires Rasip1 regulation of GTPase signaling. *Dev Cell* 20(4):526–539.
27. Saras J, et al. (1997) A novel GTPase-activating protein for Rho interacts with a PDZ domain of the protein-tyrosine phosphatase PTPL1. *J Biol Chem* 272(39):24333–24338.
28. Carey SP, Charest JM, and Reinhart-King CA (2011) Forces during cell adhesion and spreading: Implications for cellular homeostasis. *Cellular and Biomolecular Mechanics and Mechanobiology*, ed Gefen A (Springer, Berlin), pp 29–69.
29. Arthur WT, Burridge K (2001) RhoA inactivation by p190RhoGAP regulates cell spreading and migration by promoting membrane protrusion and polarity. *Mol Biol Cell* 12(9):2711–2720.
30. Ahmed SM, et al. (2012) KIF14 negatively regulates Rap1a-Radil signaling during breast cancer progression. *J Cell Biol* 199(6):951–967.
31. Ahmed SM, Daulat AM, Meunier A, Angers S (2010) G protein betagamma subunits regulate cell adhesion through Rap1a and its effector Radil. *J Biol Chem* 285(9):6538–6551.
32. Huveneers S, et al. (2012) Vinculin associates with endothelial VE-cadherin junctions to control force-dependent remodeling. *J Cell Biol* 196(5):641–652.
33. Millán J, et al. (2010) Adherens junctions connect stress fibres between adjacent endothelial cells. *BMC Biol* 8:11.
34. Xu K, Chong DC, Rankin SA, Zorn AM, Cleaver O (2009) Rasip1 is required for endothelial cell motility, angiogenesis and vessel formation. *Dev Biol* 329(2):269–279.
35. Ratheesh A, et al. (2012) Centralspindlin and α-catenin regulate Rho signalling at the epithelial zonula adherens. *Nat Cell Biol* 14(8):818–828.
36. Terry SJ, et al. (2011) Spatially restricted activation of RhoA signalling at epithelial junctions by p114RhoGEF drives junction formation and morphogenesis. *Nat Cell Biol* 13(2):159–166.
37. Pertz O, Hodgson L, Klemke RL, Hahn KM (2006) Spatiotemporal dynamics of RhoA activity in migrating cells. *Nature* 440(7087):1069–1072.
38. Kher SS, Worthylake RA (2012) Nuanced junctional RhoA activity. *Nat Cell Biol* 14(8):784–786.
39. Machacek M, et al. (2009) Coordination of Rho GTPase activities during cell protrusion. *Nature* 461(7260):99–103.
40. Smutny M, et al. (2010) Myosin II isoforms identify distinct functional modules that support integrity of the epithelial zonula adherens. *Nat Cell Biol* 12(7):696–702.